

Ain Shams University
Faculty of Medicine
Department of Radiodiagnosis

Role of Multidetector Computed Tomographic Angiography In Evaluation of Renovascular Hypertension

Submitted for Fulfillment of the Master Degree
In Radiodiagnosis

Presented By

Ahmed Mousa Qwaider

M.B, B.CH. Faculty of Medicine - Cairo University

Supervised by

Prof. Dr. Sahar Mohamed El Gaafary

Professor of Radiodiagnosis

Faculty of Medicine - Ain Shams University

Dr. Rasha Salah El Din Hussein

Lecturer of Radiodiagnosis

Faculty of Medicine - Ain Shams University

Department of Radiodiagnosis
Faculty of medicine
Ain shams University
2016



سورة البقرة الآية: ٣٢

ACKNOWLEDGMENT

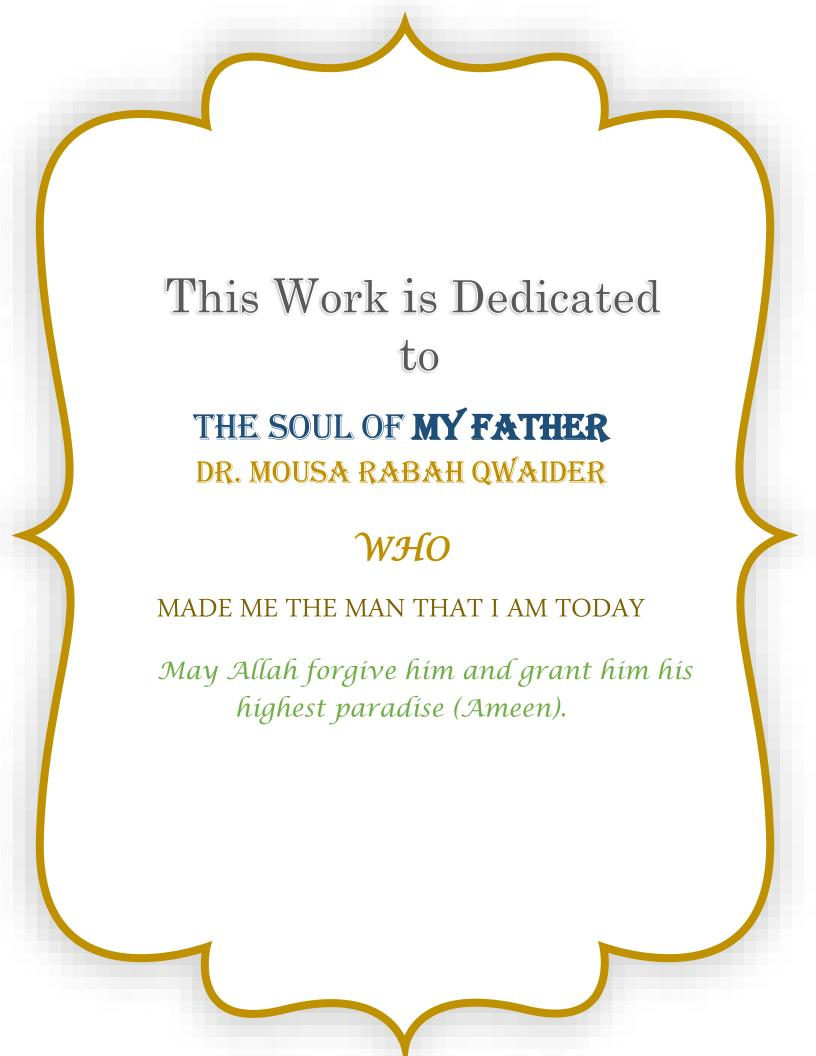
"In the name of ALLAH, the most Beneficent, the most Merciful, the most Compassionate".

First and foremost, great thanks to "ALLAH" for gifting me the ability to complete this work, without his care nothing could be achieved.

It is a great pleasure to express my deep gratitude and thanks to **Prof. Dr. Sahar Mohamed El Gaafary**, Professor of Radiodiagnosis, at Faculty of Medicine - Ain Shams University, not only for her meticulous supervision and great help throughout the study but also for her constant support, encouragement and patience to produce this work in its present form.

Many thanks and gratefulness are also forwarded to **Dr. Rasha Salah El Din Hussein,** Lecturer of Radiodiagnosis, at Faculty of Medicine- Ain Shams University, for her generous guidance, support and real cooperation. Her continuous and stimulating wise comments were very valuable.

Last but not least, I am forever indebted to my family; my great Mother, brothers and sisters; Dr. Rabah, Dr. Reham, Dr. Mohammed & Dr. Hend, who stood beside me and support me at each time of my life. Their deep faith, their prayers, best wishes and supreme trust are always the most efficient motivation to accomplish my ultimate goal. No word can describe what you have done for me. Thank you for your selfless and endless love.



List of Abbreviations

Abbreviation: Full-term

3D : Three dimensions

AAA : Abdominal Aorta Aneurysm
ACE : Angiotensin Converting Enzyme

ACR : American College of Radiology

AF : Atrial fibrillation

AHA : American Heart Association

AKI : Acute kidney injury

ALARA : As Low As Reasonably Achievable
ARAS : Atherosclerotic renal artery stenosis

ARB : Angiotensin receptor blocker

AV : Arteriovenous Shunts **AVF** : Arteriovenous Fistula

AVM : Arteriovenous Malformation

CAD : Coronary artery disease **CHF** : Congestive heart failure

CIN : Contrast Induced Nephropathy

CKD : Chronic kidney disease

CM : Contrast media

CPR : Curved planar reformattingCT : Computed Tomography

CTA : Computed Tomographic Angiography

DNA : Deoxyribonucleic acid

DSA : Digital Subtraction Angiography

FMD : Fibromuscular dysplasia **GFR** : Glomerular filtration rate

HTN : HypertensionHU : Hounsfield unitIV : Intra-venous

IVC : Inferior vena cava

mA : Milliampere

MAL : Median arcuate ligament MAS : Middle Aortic Syndrome

MDCT : Multi Detector Computed Tomography

MDCTA : Multi Detector Computed Tomographic Angiography

MIP : Maximum intensity projection

mmHg : Millimeters of mercury **MPR** : Multi-planar reformatting

MRA : Magnetic Resonance Angiography **MRI** : Magnetic Resonance Imaging

: Neurofibromatosis NF1

NSAID : Nonsteroidal anti-inflammatory drug

PAD : Peripheral artery disease **PAN** : Polyarteritis nodosa

PCE

: Peak contrast enhancement **PTA** : Percutaneous transluminal angioplasty

: Renal artery aneurysm **RAA**

RAAS : Renin Angiotensin Aldosterone System

RAD : Renal artery dissection RAS : Renal artery stenosis : Renovascular disease **RVD**

RVHT : Renovascular hypertension

SDCT : Single Detector Computed Tomography

: Second sec

: Spontaneous renal artery dissection **SRAD**

SSD : Shaded surface display : Takayasu's arteritis TA : Ultrasonography US VR : Volume rendered

List of Tables

Table No	o. Table Title	Page No.
Table 1.	Histopathological classifications and angiographic phenotypes fibromuscular dysplasia (FMD)	
Table 2.	Angiographic classification of Takayasu arteritis (TA) according extent of aortic involvement	U
Table 3.	Classification and natural history of renovascular disease (RVD	9)43
Table 4.	The probability of the existence of renovascular hypertension (RVHT).59
Table 5.	Comparisons of renal arterial studies by; computed tomography angiography (CTA), magnetic resonance angiography (MRA), ultrasonography (US) and digital subtraction angiography (DSA)	Duplex
Table 6.	Grading of renal artery stenosis (RAS)	88

List of Figures

Figure No	. Figure Title Page No.
Figure 1:	Normal CT anatomy of the perirenal fascia and spaces
Figure 2:	Illustrations of great abdominal & renal vessels relation4
Figure 3:	Illustration of Grave's classification of segmental arteries of the right kidney
Figure 4:	Section of the human kidney with a schematic representation of the microcirculation of the nephron, and tubular segments of the nephron6
Figure 5:	Diagrams of frontal coronal section illustrating major blood vessels, and Path of blood flow through renal blood vessels
Figure 6:	Normal CTA images of renal arteries; (a) MPR, (b) VR, (c) MIP9
Figure 7:	Axial MIP CTA image of normal renal veins9
Figure 8:	3D-VR renal CTA of multiple right and left renal arteries10
Figure 9:	Coronal MIP and thin MIP of renal CTA images disply one accessory hilar renal artery
Figure 10:	Renal CTA show two right renal arteries
Figure 11:	Renal MCTA; coronal MIP show 3 renal arteries & coronal VR show 2 renal arteries in the right kidney
Figure 12:	Schematic illustration & coronal VR of Circumaortic renal vein14
Figure 13:	Schematic illustration & axial CTA of Retroaortic left renal vein14
Figure 14:	Coronal VR images (anterior & posterior view) show a circumaortic left renal vein
Figure 15:	Axial & VR images show retroaortic left renal vein15
Figure 16:	Renal CTA of different cases of Renal Vein Variants15
Figure 17:	Schematic illustration of Renin Angiotensin Aldosterone System (RAAS) in blood pressure regulation

<u>List of Figures</u> (Cont.)

Figure No.	Figure Title Page No.
Figure 18:	Schematic illustration portraying the gradual transitions in renovascular disease progression over time
	Schematic illustration of Pathogenesis of renovascular hypertension in one-kidney versus two-kidney model
Figure 20:	Diagrammatic illustration of mechanism of systemic hypertension caused by renal artery stenosis
Figure 21:	Microscopic appearance of cross sections of eccentric atherosclerotic plaque and luminal occlusion causing renal artery stenosis26
Figure 22:	Microscopic pictures of medial & perimedial types of renal FMD28
Figure 23:	Schematic diagram of angiographic appearance of different pathological types of FMD; Medial, Perimedial, and Intimal fibroplasias30
Figure 24:	Microscopic appearance of biopsy from renal artery embolism31
Figure 25:	Microscopic pictures of renal artery dissection32
Figure 26:	Microscopic picture of PAN
Figure 27:	Diagrammatic scheme for angiographic classification of Takayasu's arteritis according to vessels involved
Figure 28:	Microscopic appearance of cross section from a patient with TA35
Figure 29:	Diagram illustrating different types of aneurysms38
Figure 30:	Histopathological appearance (spicemen and micrososcopic) of renal artery aneurysm39
Figure 31:	Histopathological appearance (spicemen and micrososcopic) of renal arteriovenous shunts
Figure 32:	Normal axial CT of the kidney on different scanning phases46
Figure 33:	Normal anatomy of both renal arteries & renal veins; on coronal MIP and axial renal CTA images
Figure 34:	Normal MDCTA images of both renal arteries; axial MIP, coronal VR, coronal MIP anterior and coronal MIP posterior view48

<u>List of Figures</u> (Cont.)

Figure No.	Figure Title Page No.
Figure 35:	Normal renal CTA in patient with hypertension; coronal MIP, axial MPR and VR images
Figure 36:	CPR image demonstrating saccular aneurysm at the left renal hilum 49
Figure 37:	CTA post- processing reconstruction images of the left sided RAS; coronal MIP, coronal 3D-VR and curve linear reconstructed view51
Figure 38:	A significant left sided renal artery stenosis due to atherosclerotic mural plaque is seen near the ostium on the CPR & VR images52
Figure 39:	An illustration for measuring ostial atherosclerotic RAS62
Figure 40:	Drawing illustrates measurements used to determine the degree of vascular stenosis
Figure 41:	Drawings illustrate how projection images & a cross sectional image are used to measure the diameter of an eccentric arterial stenosis63
Figure 42:	Volume rendering and MIP images of the renal arteries demonstrate high grade stenosis at the origin of the right renal artery65
Figure 43:	Coronal MIP image shows severe left RAS with poststenotic dilatation in the middle of left renal artery66
Figure 44:	Axial CTA & VR reformatted images; demonstrate an extremely shrunken left kidney fed by a very small renal artery67
Figure 45:	Axial CTA demonstrates urine CT attenuation values & DSA for patient with syphilitic aortitis show high grade bilateral stenosis with poststenotic dilatation in right main renal artery
Figure 46:	Pseudo-truncal stenosis of the renal artery (DSA. vs. CTA.)69
Figure 47:	Drawing illustrates the appearance of truncal , ostial & pseudo-truncal stenosis in the DSA and the CTA
Figure 48:	Soft plaque at the left renal artery orifice is seen by CTA71
Figure 49:	Calcified atherosclerotic plaques causing right RAS with with right renal atrophy and delayed perfusion seen on axial MIP image71

<u>List of Figures</u> (Cont.)

Figure No.	Figure Title	Page No.
Figure 50:	Axial MIP images from a CTA that performed to ass RAS in an elderly patient with hypertension	-
Figure 51:	3D-VR, curve MPR and direct axial MPR images of atherosclerotic RAS of the main right renal artery. D assessment of RAS before and after stent placement	SA images for
Figure 52:	Subvolume MIP & 3D-VR correlated with selective demonstrate "String of beads" appearance of FMD distribution of the distal two-thirds of the main renal are	in the typical
Figure 53:	Axial CTA images show expansile clot of the renal ar within the left main renal artery and near the renal sinu	•
Figure 54:	Axial CTA images demonstrate an aortic dissection fla	-
Figure 55:	right and left renal arteries	ting from false dissection flap
Figure 56:	Axial CTA, coronal CTA and VR imags demonstrate F young female patient	_
Figure 57:	MIP images & VR reformatted image demonstrate Ta findings in woman patient with a complaint of hyperten	•
Figure 58:	Axial CT, MIP and VR images demonstrate post-traumat findings in trauma patient	
Figure 59:	Axial CTA image demonstrates spastic renal arteries f hemorrhage in a patient with extensive pelvic blast injur	0 0
Figure 60:	Coronal CPR image shows saccular renal aneurysthrombus & calcification in the distal, perihilar right ren	
Figure 61:	Coronal CPR & 3D-VR CTA images demonstrate saccular aneurysms of the renal artery, respectively	
Figure 62:	Intrarenal saccular aneurysm and pseudoaneurysm is d subvolume MIP & coronal reformatted CTA images, res	•